AAS 22-616

TIDAL ATTRIBUTES OF LOW-ENERGY TRANSFERS IN THE EARTH-MOON-SUN SYSTEM

Stephen T. Scheuerle* **and Kathleen C. Howell†**

Low-energy transfers leverage multi-body dynamical structures to produce propellant efficient paths. Such trajectories often require a longer flight duration to achieve reduced propellant costs. One type of low-energy transfer in the Earth-Moon-Sun system is termed a ballistic lunar transfer (BLT). The goal of a BLT is to traverse a path from the Earth to the lunar vicinity by maintaining a reduced insertion maneuver cost. Families of BLTs that arrive into conic and multi-body orbits are constructed by leveraging structures within the bicircular restricted four-body problem (BCR4BP). Transfer solutions in the BCR4BP are employed as initial guesses when exploring paths in the higher-fidelity ephemeris model.

INTRODUCTION

Spacecraft trajectory design harmonizes the physical capabilities of a vehicle with the knowledge of the dynamical environment to reach a preferred destination in space. Recognizing the available transfer geometries and the hardware specifications is necessary in producing viable solutions. One challenge is an awareness of the underlying dynamical structures that govern a vehicle moving through any particular region in space. Expanding upon fundamental knowledge in multi-body regimes aids in the construction of desirable routes. The goal of this investigation is a characterization of the general behavior of the low-energy structures that exist in the Earth-Moon-Sun system. The motivation is relevant to the development of NASA's Artemis program, where both public and private sectors in the space industry now exhibit an increased interest in lunar missions.[1] For missions where the transfer time to the lunar region is not constrained, low-energy transfers offer propellant efficient paths. In the Earth-Moon-Sun system, one type of low-energy transfer is termed a ballistic lunar transfer (BLT). Ballistic lunar transfers leverage solar perturbations by spending several months enroute beyond the orbit of the Moon. NASA's Cislunar Autonomous Positioning System Technology Operations and Navigation Experiment (CAPSTONE) mission, that launched in June of 2022, is employing a BLT to reach the lunar vicinity later this year.[2] Multiple missions in the near-future will also leverage BLTs to reach lunar orbit, including the Korea Pathfinder Lunar Orbiter Mission (KPLO),[3] and JAXA's Equilibrium Lunar-Earth point 6U Spacecraft (EQUULEUS).[4]

*Ph.D. Student, School of Aeronautics and Astronautics, Purdue University, West Lafayette, IN 47907; sscheuer@purdue.edu

†Hsu Lo Distinguished Professor, School of Aeronautics and Astronautics, Purdue University, West Lafayette, IN 47907; howell@purdue.edu. Fellow AAS; Fellow AIAA

DYNAMICAL MODELS

Several dynamical models are employed to analyze the motion of low-energy transfers in the Earth-Moon-Sun system. The circular restricted three-body problem (CR3BP) and the bicircular restricted four-body problem (BCR4BP) are leveraged for the BLT design framework. Although the models do not represent the true motion of the Earth-Moon-Sun system, the simplifications offer insight into dynamical flow that persists in higher-fidelity models. To validate the transfer solutions constructed in this analysis, an ephemeris force model is applied. The models selected for this analysis are directly related to the separate phases of the transfer design process.

Circular Restricted Three-body Problem

Periodic orbits in the CR3BP offer sample destinations in cislunar space for low-energy transfers. The CR3BP depicts the motion of a spacecraft (P_3) due to the gravitational influence of the Earth and Moon (P_1 and P_2). It is assumed the mass of the spacecraft is negligible compared to the primary bodies, thus, the motion of the Earth and Moon is independent of the spacecraft. The Earth and Moon are then assumed to follow circular orbits around their mutual barycenter (B_1). The mass of the Earth and Moon are M_1 and M_2, respectively. The CR3BP is nondimensionalized to simplify the equations of motion and aid in numerical tolerance. The characteristic length and time are defined such that the nondimensional distance between the two primary bodies is one, and the mean motion of the P_1-P_2 system is unity. Expressing the equations of motion in a coordinate frame that rotates with the primary bodies, the differential equations are time-independent.[5] The motion of the spacecraft (P_3) is described by three scalar nonlinear second-order differential equations, that are expressed as,

$$\ddot{x} = 2\dot{y} + \frac{\partial U}{\partial x} \qquad \text{(1a)} \qquad \ddot{y} = -2\dot{x} + \frac{\partial U}{\partial y} \qquad \text{(1b)} \qquad \ddot{z} = \frac{\partial U}{\partial z} \qquad \text{(1c)}$$

where x, y, z and $\dot{x}$, $\dot{y}$, $\dot{z}$ are the position and velocity components of the spacecraft in the Earth-Moon rotating frame. The variables $\frac{\partial U}{\partial x}$, $\frac{\partial U}{\partial y}$, and $\frac{\partial U}{\partial z}$ are the partial derivatives of the pseudo potential function U with respect to the position of P_3. The pseudo-potential function, U, is written as,

$$U = \frac{1}{2}\left(x^2 + y^2\right) + \frac{1-\mu}{r_{13}} + \frac{\mu}{r_{23}} \tag{2}$$

where the term μ is the mass parameter, defined $\mu = \frac{M_2}{M_1+M_2}$. The value r_{ij} is the scalar distance between body i and j. The CR3BP possesses a single integral of the motion. The existence of an integral of the motion offers a constant energy metric along a ballistic trajectory. The integral of the motion is denoted the Jacobi Constant, and remains fixed along a ballistic arc.[6] The Jacobi Constant value (C) is written as,

$$C = 2U - (\dot{x}^2 + \dot{y}^2 + \dot{z}^2) \tag{3}$$

The Jacobi constant represents as an 'energy-like' quantity, consisting of a pseudo-potential term and the norm of the rotating velocity components. As the velocity terms are negative, an increase in the Jacobi Constant corresponds to a decrease in energy. For trajectories in the CR3BP, the Jacobi Constant adds insight in applying dynamical systems theory, including a basis for comparing two transfer energies, and assessing bounded regions for a given energy level.

Bicircular Restricted Four-body Problem

The BCR4BP governs the motion of a spacecraft in the Earth-Moon-Sun system. The first two assumptions in the BCR4BP are similar to that of the CR3BP. The mass of the spacecraft (P_3) is negligible compared to the mass of the Earth, Moon, and Sun (P_1. P_2, and P_4). The Earth and Moon are assumed to follow circular orbits about their mutual barycenter (B_1). The star-planet-moon system is defined by assuming the Sun and the Earth-Moon system follow circular orbits about the total system barycenter (B_2). The motion of a spacecraft with respect to the primary bodies (Earth, Moon, and Sun) may be expressed in either an Earth-Moon or Sun-B_1 rotating frame. A schematic illustrating the two rotating coordinate frames is represented in Figure 1. To differentiate between the Earth-Moon rotating frame in the CR3BP and the BCR4BP, the Earth-Moon rotating quantities in the BCR4BP are defined with tildes overhead, i.e., $(\widetilde{x}, \widetilde{y}, \widetilde{z})$. Likewise, the BCR4BP Sun-B_1 rotating frame is defined with underlined-quantities, i.e., $(\underline{x}, \underline{y}, \underline{z})$. Similar to the CR3BP, the model may be nondimensionalized by the respective rotating frames. For this analysis, the system is nondimensionalized by the Earth-Moon quantities. The distance to the Sun is determined using the characteristic length in the Earth-Moon system. The equations of motion for P_3 in the BCR4BP are formulated relative to the Earth-Moon rotating frame, as

$$\ddot{\widetilde{x}} = 2\dot{\widetilde{y}} + \frac{\partial \Upsilon}{\partial \widetilde{x}} \quad \text{(4a)} \qquad \ddot{\widetilde{y}} = -2\dot{\widetilde{x}} + \frac{\partial \Upsilon}{\partial \widetilde{y}} \quad \text{(4b)} \qquad \ddot{\widetilde{z}} = \frac{\partial \Upsilon}{\partial \widetilde{z}} \quad \text{(4c)}$$

where Υ is the pseudo-potential function for the differential equations in the BCR4BP as represented in the Earth-Moon rotating frame. The pseudo-potential function is expressed in terms of the orientation of the Sun in the rotating frame, and written as

$$\Upsilon = \frac{1}{2}(\widetilde{x}^2 + \widetilde{y}^2) + \frac{1-\mu}{r_{13}} + \frac{\mu}{r_{23}} + \frac{\widetilde{m}_S}{r_{43}} - \frac{\widetilde{m}_S}{a_S^2}(\widetilde{x}\cos(\theta_S) + \widetilde{y}\sin(\theta_S)) \quad (5)$$

where m_S is the nondimensional mass of the Sun, i.e., $m_S = \frac{M_4}{M_1+M_2}$, a_S is the constant radius between the Sun and Earth-Moon barycenter that describes the circular motion of the Sun-B_1 system, and r_{43} is the scalar distance from the Sun to the spacecraft. The angle that orients the Sun in the Earth-Moon rotating frame is defined as the Sun Angle (θ_S), and is illustrated in Figure 1(a). In the Sun-B_1 rotating coordinate frame, the Earth-Moon angle (θ_{EM}) orients the Earth and Moon line with respect to the Sun as apparent in Figure 1(b).

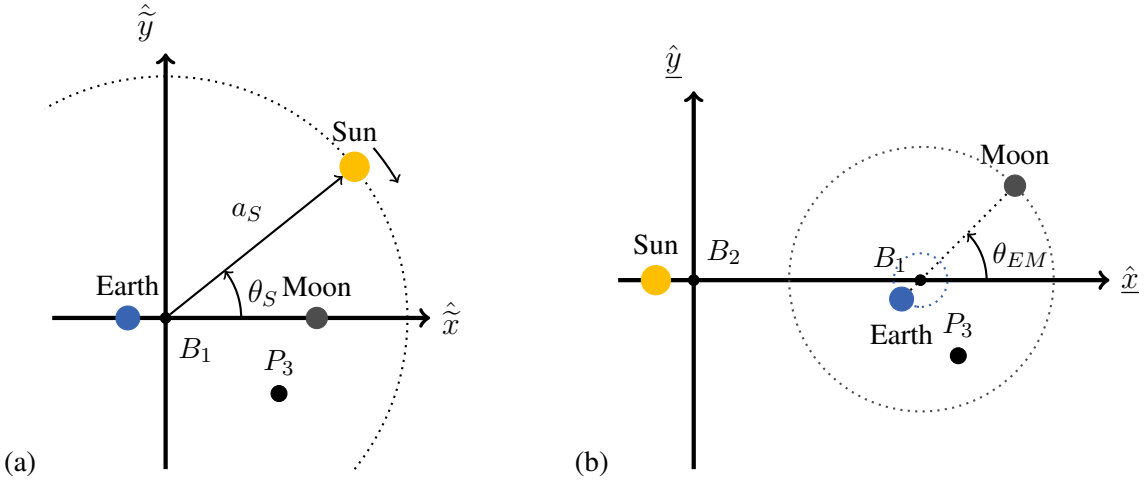

Figure 1: The Earth-Moon (a) and Sun-$\boldsymbol{B_1}$ (b) rotating coordinate frames

In the Earth-Moon-Sun system, the motion of the Sun does not actually remain in the Earth-Moon plane for all time. But for this analysis, it is adequate to assume that the motion of the Earth, Moon, and Sun are coplanar, i.e., the orbital plane of the Earth and Moon lies in the ecliptic plane. The BCR4BP is time-dependent as the model relies on the relative motion of the Sun-B_1 and Earth-Moon systems. With the coplanar assumption, the Sun angle is periodic over the synodic period of the Earth-Moon-Sun system. By incorporating the motion of all three primaries, the BCR4BP serves as an effective model for generating BLTs.[7]

Ephemeris Force Model

The N-body ephemeris force model incorporates the ephemerides of the astronomical bodies to predict the governing motion of a spacecraft. The goal in mission operations is the use of a high-fidelity model to mimic the motion of a spacecraft through the complex dynamical regime. Although the CR3BP and BCR4BP are multi-body dynamical environments, the assumptions render the models as incoherent. To minimize those differences between models and reality, the N-body ephemeris force model is also available. Consider N bodies denoted as P_1, P_2, ..., P_N, all modeled as point masses. It is advantageous to describe the motion of an object with respect to an astronomical body, such as the Earth or Moon. Therefore, a central body P_C is selected as the origin of the inertial reference frame. For this analysis, the Earth is used as the central body, and the ephemerides of the Earth, Moon, and Sun are incorporated to describe the motion of the spacecraft. Recall P_3 is the body associated with the spacecraft, while P_1, P_2, and P_4 refer to the Earth, Moon, and Sun, respectively. To simplify the nomenclature for the expression, the relative position of body i with respect to the central body is written as $\bar{r}_i$, where for the spacecraft, $i = 3$. The motion of the spacecraft in the N-body ephemeris model is then evaluated from the governing equations of motion,

$$\ddot{\bar{r}}_3 = -G\frac{M_1}{r_3^3}\bar{r}_3 - G\sum_{\substack{j=1 \\ j\neq 1,3}}^{N} M_j\left(\frac{\bar{r}_3 - \bar{r}_j}{|\bar{r}_3 - \bar{r}_j|^3} + \frac{\bar{r}_j}{r_j^3}\right) \tag{6}$$

where G is the gravitational constant. Recall that the quantity M_i is the mass of the body i, e.g., M_1 is the mass of the Earth (P_1). The structure of Equation (6) incorporates the influence of the spacecraft due to the central body as well as perturbing bodies. Although Equation (6) governs motion of the spacecraft, it does not alone guarantee a valid high-fidelity model. The increase in fidelity from the CR3BP or BCR4BP to the ephemeris model originates from the ephemerides of the bodies. The terms $\bar{r}_j$ describe the position of an astronomical body with respect to the central body. Therefore, by leveraging the ephemerides of the Earth, Moon, and Sun at a given epoch, a useful higher-fidelity model emerges. The ephemerides in this analysis are accessed from the Jet Propulsion Laboratory DE430 data set.[8] The Earth, Moon, and Sun are selected as the only governing bodies, reflecting their predominant influence on the geometry of ballistic lunar transfers. Additional perturbations due to other planets, solar radiation pressure, or spherical harmonics also influence the trajectories explored in this analysis, but are not incorporated in this investigation.

Naturally, there are advantages and disadvantages to leveraging the ephemeris model. The validation and accuracy as compared to the true motion is a key benefit. Thus, for mission preparation and planning, an ephemeris model aids in validating trajectory designs and creating a baseline framework for operations. However, as the motion of the astronomical bodies are no longer periodic, a challenge exists in recognizing any underlying dynamical structures. In addition, the ephemeris force model may require additional computational resources and time. In this investigation, how-

ever, the N-body model demonstrates a procedure for transferring solutions generated in the CR3BP and BCR4BP to a higher-fidelity ephemeris model.

BALLISTIC LUNAR TRANSFERS IN THE BCR4BP

The BCR4BP models the influence of the Sun on transfers in the vicinity of the Earth-Moon system. Previous analysis by the authors explores strategies for producing planar families of BLTs to conic and multi-body orbits in the BCR4BP.[9,10] As the BCR4BP models the end-to-end geometry of a BLT, point-solutions initiate a continuation along desired constraint directions to illuminate a range of viable transfer options. New strategies for constructing ballistic lunar transfers are explored in this investigation.

Transfer Families to Spatial Conics

Families of ballistic lunar transfers provide insight into the available low-energy paths between the Earth and Moon. Past analyses by the authors have explored several techniques for constructing planar ballistic lunar transfers to conic orbits in the BCR4BP.[7,9] Such approaches deliver families of transfers with fixed properties to meet mission specific constraints. Examples include families of transfers with fixed time-of-flight, initial Sun angle, trans-lunar injection cost (TLI), or lunar orbit insertion (LOI) cost. For trajectory design, recognizing mission constraints and hardware capabilities directly impacts the type of geometry available. Moving transfers into the third dimension expands the solution-space and also enables new types of constraints that can be accommodated.

Characterizing BLTs enable construction of a framework for generating families of transfers. Previous investigations detail procedures to produce an initial guess for a BLT.[7] Several continuation strategies exist for expanding the initial guess into a family of transfers. The approach incorporated into this analysis is pseudo-arclength continuation. Pseudo-arclength continues the family along a non-physical parameter that steps along the null-space of the Jacobian matrix. To accomplish the continuation process requires a number of physical constraints, modeled as scalars and equal to one less than the number of scalar free variables. For example, if there are six free variables in the differential corrector, then five physical constraints are applied, alongside the pseudo-arclength step constraint. Additional details regarding the pseudo-arclength strategy employed is outlined by the authors previously.[7] When developing a family of BLTs, careful selection of targeting constraints is critical for the resultant paths.

When constructing a family of BLTs, careful selection of targeting constraints is critical the resultant paths. The first constraint is that the transfer originates at an altitude of 150 km above the surface of the Earth. The initial state is also constrained to be a perigee, such that the trans-lunar injection (TLI) maneuver is tangential to the velocity near the Earth. The initial state is then post-TLI. The next constraints are associated with the arrival condition at the Moon. Two similar conditions must be met, i.e., the final state is at a 100 km altitude above the surface of the Moon. The final state must also be a perilune. Any lunar orbit insertion (LOI) costs assume that the insertion orbit is a 100 km altitude, circular orbit. Injection and insertion costs may be less expensive for missions that desire to depart from or arrive into elliptical orbits. Circularizing the orbit is selected for this analysis as a basis of comparison across a variety of transfer families. The entire transfer from Earth departure to arrival at the Moon is ballistic, therefore, a state is fully defined by eight variables. These variables include the typical six-element state vector, the initial Sun angle, and the time-of-flight. In the planar case, the $\widetilde{z}$ and $\dot{\widetilde{z}}$ terms are zero, providing six free variables rather than eight. With the two altitude and two apse constraints, only one additional constraint is necessary

to generate a family of BLTs in the planar problem. However, for spatial BLTs, three constraints are necessary to construct a family with the pseudo-arclength continuation scheme. The constraints may be some combination of timing, maneuver magnitude, epoch, or inclination of the conic orbits. The inclination is defined with respect to the Earth-Moon orbital plane, and is written as the variable γ. The inclination γ is evaluated as the angle between the positive $\hat{\bar{z}}$-axis and the instantaneous specific angular momentum of the spacecraft trajectory with respect to the orbiting body. For example, the instantaneous specific orbital angular momentum of the spacecraft about the Moon is,

$$\bar{h} = \begin{bmatrix} h_x & h_y & h_z \end{bmatrix} = \bar{r}_{23} \times \bar{v}_{23} \tag{7}$$

Recall the term $\bar{r}_{23}$ refers to the position vector from the Moon to the spacecraft. As the Moon is fixed in the Earth-Moon rotating frame, the velocity vector $\bar{v}_{23}$ is equivalent to the velocity of the spacecraft with respect to the barycenter. The terms h_x, h_y, and h_z are the projections of the angular momentum vector onto the rotating coordinate axes. Therefore, the angle between the angular velocity vector and the $\hat{\bar{z}}$-axis is,

$$\gamma = \arccos\left(\frac{h_z}{||h||}\right) \tag{8}$$

For planar transfers where the angular momentum vector is entirely in the $\hat{\bar{z}}$ direction, Equation (8) yields an inclination of zero. Note that arccosine returns angles between zero and 180°. For inclinations from 0-90°, the orbit is traversing prograde with respect to the central body. Retrograde motion is represented by inclination angles between 90-180°. With a definition for the inclination at the arrival conic orbit, such a constraint may be introduced to construct families of spatial BLTs in the BCR4BP. Consider a sample transfer as depicted in Figure 2. The plot illustrates the $\underline{\hat{x}}\underline{\hat{y}}$-projection of a BLT in the Sun-B_1 rotating coordinate frame. The transfer has a flight duration of 180-days from TLI to LOI. The TLI maneuver magnitude to depart from a 150 km altitude Low Earth Orbit (LEO) is 3,217 m/sec, while the LOI maneuver magnitude is 660 m/sec. For a basis of comparison, previous investigations have approximated the theoretical minimum LOI in a range from 622 to 626 meters per second for similar transfer geometries.[7,9,11] The transfer arrives into a Low Lunar Orbit (LLO) with an altitude of 100 km, and an 85-degree inclination γ. The epoch for LOI is a new Moon, i.e., the Sun angle is zero ($\theta_S = 0$). The process for producing the initial transfer is outlined in previous investigations, and employs periapse Poincaré mapping techniques.[9,12] The transfer spends most of the time traversing through through quadrants II, III, and IV. A family of BLTs is constructed in the BCR4BP through pseudo-arclength continuation. The transfer illustrated in Figure 2 serves as the initial guess to generate the family of transfers. To develop the set of constraints necessary for the continuation strategy, assume the arrival conditions at the Moon are fixed, that is, the arrival epoch ($\theta_S = 0$), LOI maneuver magnitude (660 m/sec), and inclination ($\gamma = 85$ degrees) remains constant across all members of the family. As the final epoch is fixed, and the initial epoch is varied, the overall time-of-flight along the transfer evolves with the family. The $\underline{xy}$-projection of a family of BLTs is illustrated in Figure 3. Each arc is a unique transfer that departs from a 150 km altitude LEO, and arrives into the desired insertion constraints. The TLI maneuver magnitude varies from 3,201 m/sec to 3,233 m/sec across the family.

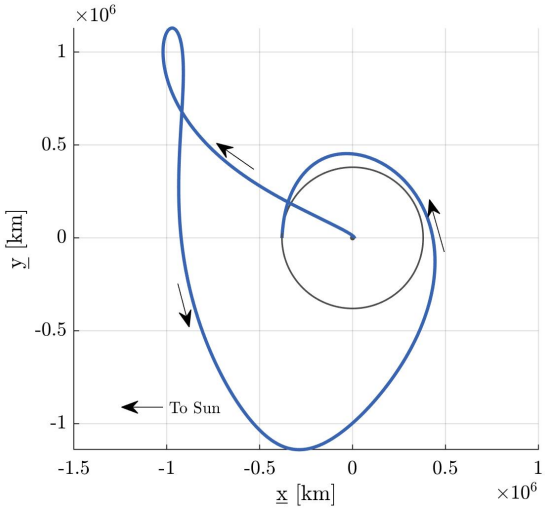

Figure 2: Sample BLT in the BCR4BP with a 180-day time-of-flight and a LOI of 660 m/sec. The arrival orbit is a 100 km altitude LLO, with an 85-degree inclination (γ)

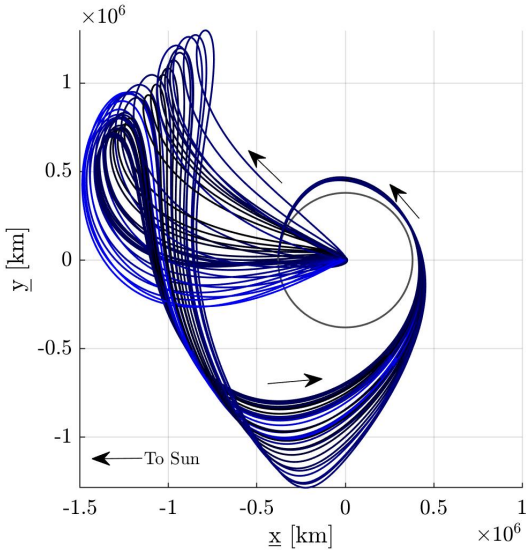

Figure 3: Family of BLTs in the BCR4BP with a LOI of 660 m/sec. The arrival orbit is a 100 km altitude LLO with an 85-degree inclination (γ)

By comparing Figure 2 to Figure 3, the family offers several solutions that extend across the Sun-B_1 rotating frame. Recall that all the transfers in Figure 3 arrive into similar LLOs, with the only difference being the arrival right ascension in the rotating frame. To describe the available transfers among the members of the family, the evolution of the initial Sun angle is represented in Figure 4. The figure reflects the progression of time-of-flight in terms of the initial epoch and, thus, for each transfer. The first observation from Figure 4 is that members of the family exist through all values of initial Sun angle. Recall that, in the BCR4BP, the Sun angle is related to the epoch, or orientation of the Earth-Moon-Sun system. Therefore, there is a member of the family for all possible epochs.

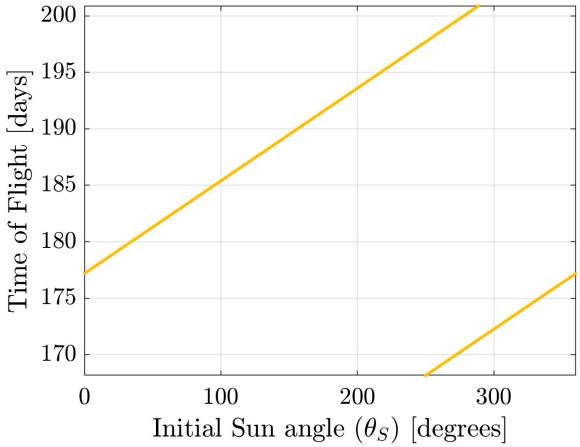

Figure 4: Time-of-flight as a function of the initial Sun angle for the family of BLTs as viewed in Figure 3

Rather than a fixed arrival epoch, it is often advantageous to investigate a range of possible transfer scenarios for a fixed launch epoch. Consider a sample set of constraints to evaluate a range of viable transfers. The first four constraints on the transfers are consistent with the altitude and apse constraints previously identified. The fifth constraint corresponds to the initial epoch for the transfer, i.e., a given launch date. The initial epoch is based on the initial guess, that is, a Sun angle of 233 degrees. The sixth constraint represents a limitation on the spacecraft insertion maneuver; the LOI maneuver is fixed to 640 meters per second. Finally, assume that the arrival inclination into the LLO is 45 degrees. A family of transfers that fulfill all of the constraints appears in Figure 5. Each individual line represents a different member of the family, where the darker blue lines identify the longer time-of-flight. The black circle represents the orbit of the Moon, and the Moon travels counterclockwise in the Sun-B_1 rotating frame. The TLI maneuver costs as a function of the

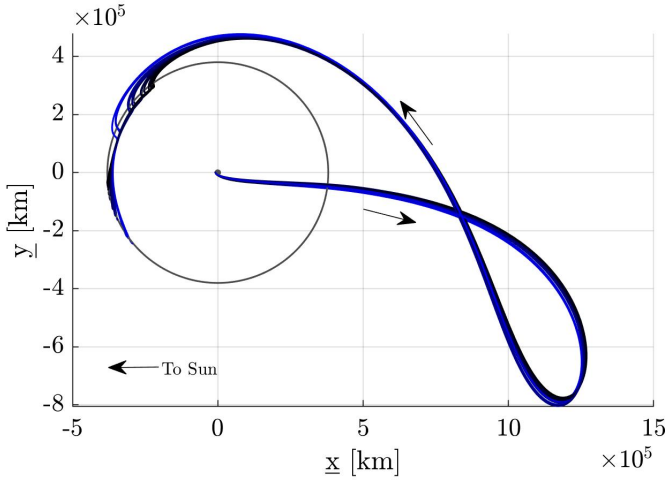

Figure 5: Family of BLTs in the BCR4BP with a LOI of 640 m/sec. The arrival orbit is a 100 km altitude LLO with an 45-degree inclination (γ)

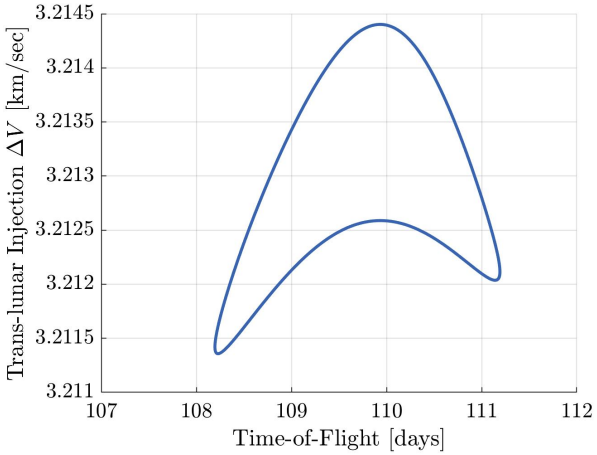

Figure 6: Evolution of the TLI maneuver cost and the time-of-flight across the members of the family illustrated in Figure 5

time-of-flight associated with the family in Figure 5 are illustrated in Figure 6. As is apparent, the family renders a closed curve, with roughly a 3 m/sec variation in the TLI maneuver, and a difference of three days between the shortest and longest time-of-flight. Recall each transfer departs the Earth from precisely the same epoch.

Knowledge of the surrounding structures emerges through natural parameter continuation process across families. For the sample family in Figure 5, each member of the family arrived into a LLO with an inclination (γ) of 45 degrees. Assume that constraint is now free to vary, additional families of transfers at different inclinations are constructed. Two families each with a different arrival inclination with respect to the Earth-Moon orbital plane are illustrated in Figure 7. As each family has a different arrival inclinations, the values are set to 5 degrees, and 25 degrees for Figure 7(a) and Figure 7(b), respectively. For the transfers that arrive into a lower inclination LLO, the transfer geometry relative to the the Sun-B_1 rotating frame remains consistent. The evolution of time-of-flight and TLI maneuver magnitude across the three families is illustrated in Figure 8. The 5 degree,

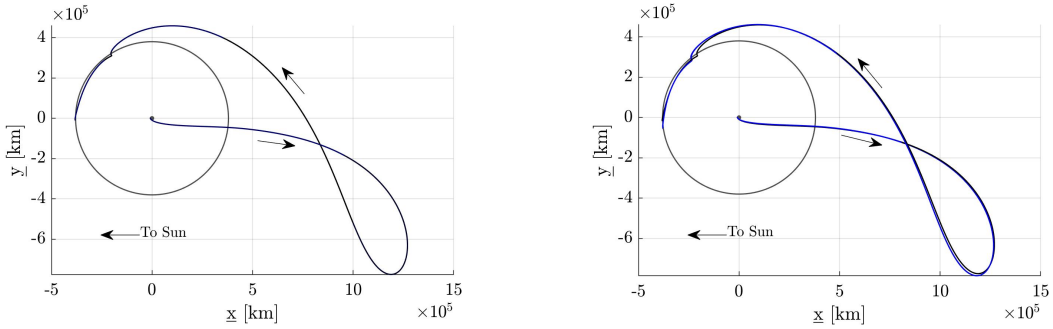

Figure 7: Families of BLTs in the BCR4BP with a LOI of 640 m/sec, with each family having a different arrival inclination (γ): (a) 5 degrees, (b) 25 degrees

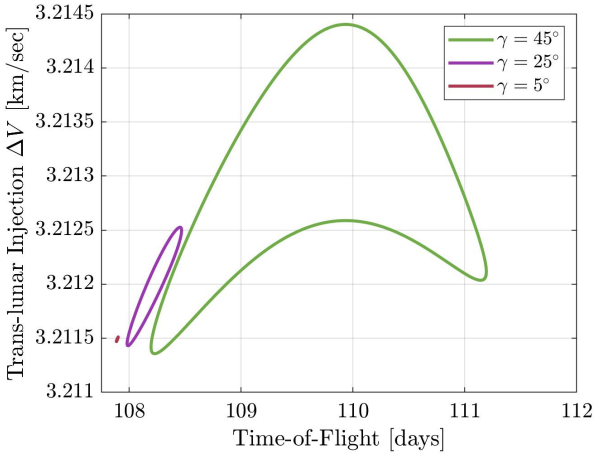

Figure 8: Evolution of the TLI maneuver cost and the time-of-flight across fixed inclination families

25 degree, and 45 degree families are represented in Figure 8 as the red, violet, and green curves, respectively. Note that as the arrival LLO inclination decreases across the families, the range of possible solutions is reduced. By exploring transfers that arrive into higher inclination LLOs, a wider range of transfer solutions emerge. A similar process is repeated for transfer families that arrive into LLOs with 65 and 85 degree inclinations. The paths in the Sun-B_1 coordinate frame for the 65-degree family and the 85-degree family are illustrated in Figures 9(a) and 9(b), respectively. Recall that each transfer has the same initial Sun angle, LEO altitude of 150 km, LLO altitude of 100 km, and the same LOI maneuver cost of 640 m/sec. For each family in Figure 9, the longer time of flight transfers correlate to a more blue arc. One pattern that emerges between the families in Figure 7 and Figure 9 is that a wider range of transfer geometries become available when the inclination γ increases. The transfers in Figure 7(a) that arrive at $\gamma = 5$ degrees appear to overlap each other closely in the Sun-B_1 rotating frame, almost appearing as one transfer. Whereas the transfers in Figure 9(b) spread across a wider range of the region, and arrive near the Moon at different epochs. As each transfer departs from the Earth at the same starting epoch, the initial departure direction away from the Sun is consistent. The major differences occur upon arrival into cislunar space, where some transfers spend more time in the vicinity of the Moon prior to insertion into the LLO. A comparison is also seen between Figure 5 and Figure 9. Since the family illustrated in Figure 5 has an inclination of $\gamma = 45$ degrees, with the same remaining constraints, it falls into the inclination range between Figure 7(b) and Figure 9(a). It is advantageous to examine the variation in flight duration and TLI maneuver costs for the higher inclination LLOs, adding to the curves in Figure 6 and Figure 8. Each curve in Figure 10 corresponds to a different family of BLTs that arrive into the LLO with a specified inclination. The entire region encompassed by the families is represented in Figure 10(a), a zoomed version of the plot appears in Figure 10(b). The blue curve is defined by an arrival inclination of 85°, and covers the largest range across time-of-flight and TLI maneuver magnitude. The small red curve in Figure 10(b) corresponds to the family with the smallest inclination value of 5°, and is the same 5° curve as Figure 8. As observed from Figure 7 and Figure 9, as the arrival inclination increases from 5 to 85°, the range of available paths in the family also increases. By continuing the families through inclination, and updating the initial guess, a wider set of possible transfers become available. As the family corresponding to the 85-degree inclination expands through Figure 10(a), several lobes emerge suggesting that

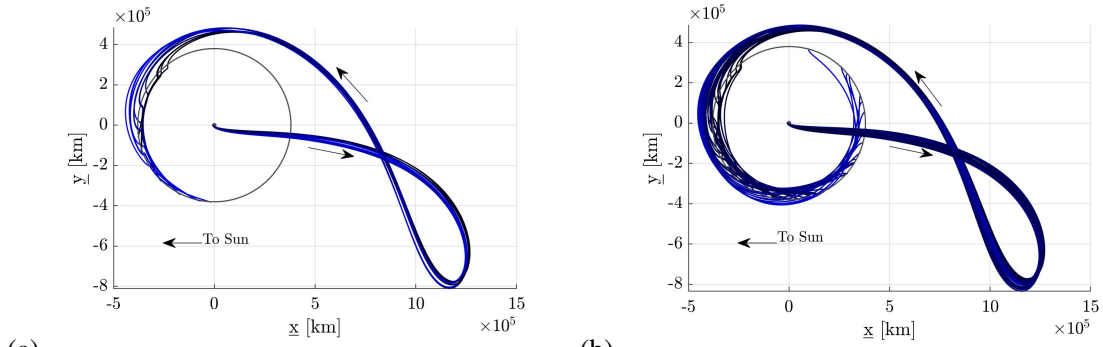

Figure 9: Families of BLTs in the BCR4BP with a LOI of 640 m/sec, with each family having a different arrival inclination (γ): (a) 65 degrees, (b) 85 degrees

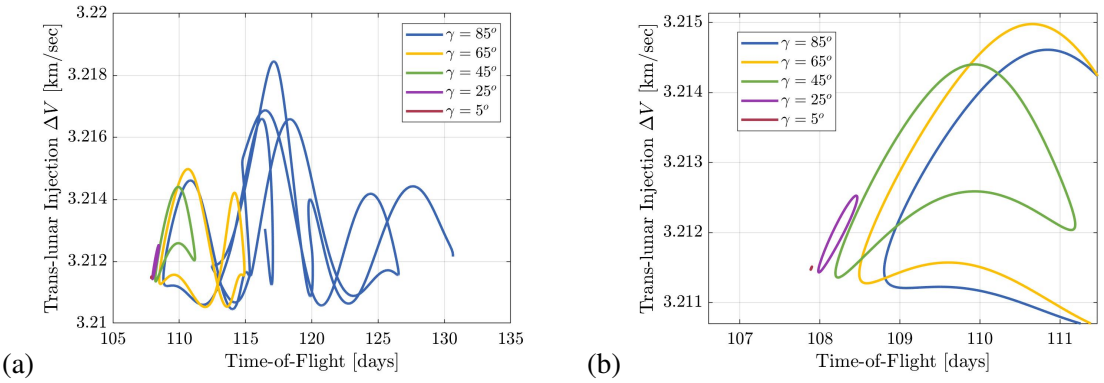

Figure 10: Progression of TLI and flight duration for the five families of BLTs with different arrival inclination (γ) values: (a) full plot (b) zoomed in on smaller inclinations

additional transfers may exist. Due to the pseudo-arclength continuation strategy, the closed curves represented by the red, magenta, green, and yellow curves in Figure 10 continue along a path defined by the constraints. Clearly, the continuation process is highly dependent on the selection of an initial guess. By selecting an alternative initial guess from a solution on the 85-degree blue curve from Figure 10, a natural parameter continuation scheme along a new family is applied, gradually reducing the arrival inclination. This approach reveals a wider range of BLT solutions, as illustrated in Figure 11. Note that each curve represents a different family of BLTs, with the same initial Sun angle and arrival LOI maneuver constraints. The difference between each family is the arrival inclination, described by the color of the lines. The darker blue colors are lower inclination, and appear to collapse to a single point. Due to the dimensionality of the problem, once the family collapses to an inclination of zero, the problem is now fully-determined, and only a localized point solution exists. Conversely, as noted previously, the higher inclination curves cover a wide range of the available space. From an initial glance, a low-inclination LLO may offer a reduced range in transfer opportunities from the Moon. However, by analyzing transfers to higher inclination LLOs, more solutions emerged that might otherwise go undetected with the previous continuation process.

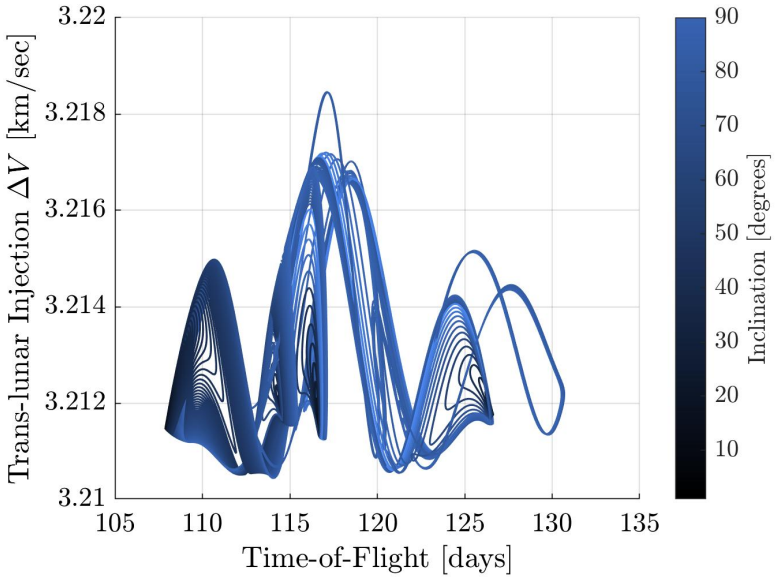

Figure 11: Progression of TLI and flight duration for many families of BLTs with different arrival inclination (γ)

Transfer Families to Multi-body Orbits

Known traits from the CR3BP may be leveraged to generate BLTs in the BCR4BP. One of the major advantages to low-energy transfers is the reduced insertion costs required upon arrival in the vicinity of the Moon. Low-energy transfers are attractive to small satellite missions with their potential for bounded behavior about the Moon without a large maneuver. As the Jacobi constant corresponding to multi-body orbits is generally lower than that of conic orbits about the Moon, these complex structures become desirable for missions with tight constraints on fuel requirements. Several previous investigations have explored techniques for generating paths to multi-body orbits. Parker et al. explore methods in dynamical systems theory to construct such transfers.[13] McCarthy investigates BLTs that deliver spacecraft into quasi-periodic orbits.[14,15] These previous authors construct transfers within the BCR4BP, including application to a 9:2 Near Rectilinear Halo Orbit (NRHO).[9,10] This current analysis builds upon the BCR4BP and periodic orbits from the CR3BP to offer a wider range of solutions.

Periodic orbits from the CR3BP introduce new low-energy transfer geometries to the Moon. One challenge with the BCR4BP is the time-dependency within the model. Periodic orbits only exist when the period of the orbit is resonant with the Earth-Moon-Sun system. This resonance constraint reduces the number of periodic orbits that exist within the model. The challenge arises when selecting a destination orbit in the BCR4BP because the number of options are limited in comparison to the CR3BP. Previous strategies have leveraged manifold structures associated with period orbits in the BCR4BP.[9,10] It is observed that each periodic orbit only offers a select number of BLTs that traverse from the Earth to the periodic orbit. There are several advantages to using periodic orbits from the BCR4BP. First, the paths are truly ballistic post-TLI, requiring no insertion maneuver to enter the orbit. The second advantage is actually the epoch dependency of the manifold arc. Although an added dependency may appear as a disadvantage, in practice, the manifold arc is

arriving into an orbit with an inherent constraint on the Sun angle. However, arriving at a fixed phase is not necessary for all missions scenarios, nor is an orbit resonant with the synodic period. Therefore, this investigation introduces a new alternative technique to construct BLTs to periodic orbits in the BCR4BP. The concept incorporates the technique to transition the final solution to the ephemeris force model. Experience suggests that many periodic structures in the Earth-Moon CR3BP transition well to the ephemeris force model.[16] The alternate approach leverages states from a periodic orbit in the CR3BP as the target conditions for low-energy transfers in the BCR4BP. Both the CR3BP and the BCR4BP are formulated in an Earth-Moon rotating frame. Due to the solar perturbations in the BCR4BP, the dynamics between the two models are not the same. A periodic orbit state from the CR3BP does not produce a periodic orbit in the BCR4BP, and slightly diverges from the desired path. The targeting strategy is then similar to the scheme described in the previous section on BLTs to conic orbits. The first two constraints remain the same, where the transfer originates at a LEO with an altitude of 150 km, and the initial state on the transfer is a perigee. The remaining constraints target the Earth-Moon rotating position and velocity states along a periodic orbit from the CR3BP. As previously introduced, a planar BLT is defined by six states, including the position and velocity, as well as as the time-of-flight and the initial Sun angle in the BCR4BP. With the two initial constraints, and the four state variables corresponding to a planar periodic orbit, the problem is fully-determined. To construct a family of BLTs that arrive at a periodic orbit, a new variable must be introduced. One potential variable that describes the location along the periodic orbit with respect to some initial condition, as in the schematic represented in Figure 12. The blue curve is an arbitrary periodic orbit, where the black arrows indicate the direction of motion. The red dot corresponds to the initial state defining the periodic orbit, typically on the x-axis. The variable τ represents the time beyond the initial state that reaches a target location along the curve. Thus, the target location for the graphic is the green dot. As the periodic orbit is a curve, allowing τ to vary during the continuation process enables the construction of a family of BLTs to a three-body periodic orbit.

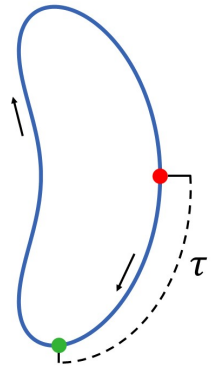

Figure 12: Graphic representation of the variable τ

Consider a sample scenario to construct a family of transfers to a L2 Lyapunov orbit. The selected Lyapunov orbit is periodic in the CR3BP, with a period of roughly 15.3 days. By employing a pseudo-arclength continuation strategy, alongside the variation in τ as the target location along the orbit, a family of BLTs in Figure 13 is constructed. Each curve represents a different transfer, where a shorter time-of-flight corresponds to a transfer that is evolving toward a blue color. The same family of transfers is represented in Figure 14 in the Earth-Moon rotating frame. The motion

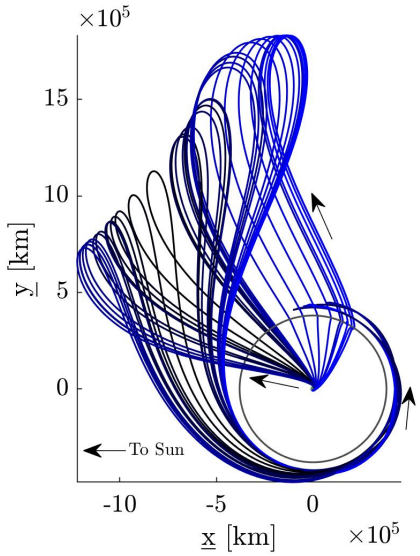

Figure 13: Family of BLTs in the BCR4BP that insert into a L2 Lyapunov Orbit from the CR3BP, illustrated in the Sun-$\boldsymbol{B_1}$ rotating frame

near the Moon includes both outbound lunar passes and the arrival dynamics inserting into the L2 Lyapunov orbit. The closest approach to the center of the Moon is roughly 1700 km, therefore, a small portion of the transfers impact the lunar surface during the outbound flyby. The TLI maneuver magnitude is plotted as a function of the initial Sun angle in Figure 15. The TLI magnitude varies by 75 m/sec, where transfers with a lower TLI leverage an outbound lunar flyby. Another family trait highlights the fact that a transfer solution exists for each initial Sun angle. Therefore, for this family to the L2 Lyapunov orbit, a transfer solution exists for any initial epoch.

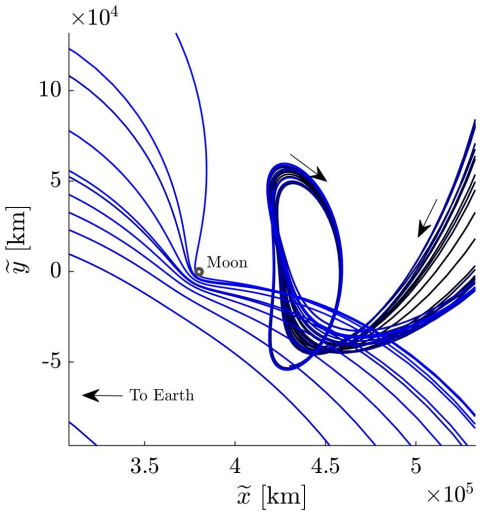

Figure 14: Family of BLTs in the BCR4BP that insert into a L2 Lyapunov Orbit from the CR3BP, illustrated in the Earth-Moon rotating frame near the Moon

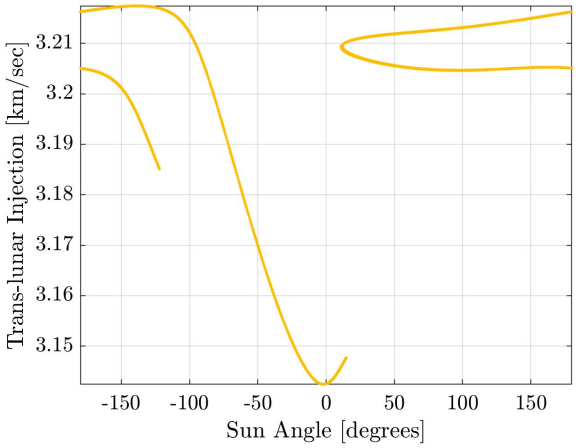

Figure 15: Evolution of TLI maneuver magnitude in terms of initial Sun angle along the family of transfers illustrated in Figure 14

TRANSITIONING TRANSFERS TO THE EPHEMERIS MODEL

Solutions constructed in the BCR4BP model serve as an initial guess for transitioning to a higher-fidelity model. Although the BCR4BP incorporates the influence of the Earth, Moon, and Sun into one model, there are multiple assumptions that do not fully represent the complex dynamics. For actual implementation of a BLT, a higher-fidelity model is necessary to accurately accommodate the motion of the bodies. The ephemerides of the Earth, Moon, and Sun are incorporated into a N-body model to depict the motion of the spacecraft at higher precision. One challenge with the ephemeris model is the lack of periodicity, therefore, transfer solutions are epoch-specific. A benefit to the CR3BP and BCR4BP is the periodicity of the models. An initial guess in the CR3BP is valid for any epoch, as the model is time-independent; in the BCR4BP, solutions exist for a specific orientation of the Sun (θ_S). Although a transfer in the BCR4BP remains time-dependent, the Earth-Moon-Sun structures repeat each synodic month. When transitioning a solution from the BCR4BP to the ephemeris model, similar structures should emerge in resonance with the Earth-Moon-Sun synodic period. For a family of BLTs in the BCR4BP, the range of initial Sun angles directly relates to the accessible starting epochs for the ephemeris model, i.e., launch opportunities.

Several strategies are simultaneously required to transition a transfer from the BCR4BP to the ephemeris force model. Note that the Earth-centered, Earth-equatorial, J2000 reference frame is selected as the inertial coordinate system for this analysis. The first step to transition a solution requires the proper selection of the initial epoch. As the Sun angle orients the position of the Sun in the BCR4BP, a similar orientation appears in the ephemeris force model. Boudad explores a process for converting the Sun angle in the BCR4BP to an ephemeris epoch.[17] Since the Sun angle repeats every synodic month, an initial guess is necessary as an approximate time for the origin of the transfer, i.e., a starting month and year. Conversely, if a specific starting epoch is identified for the mission, then a corresponding Sun angle is calculated. A schematic representing the Sun angle with an inclined lunar orbit is represented in Figure 16. The illustration in the Sun-B_1 rotating frame, where the motion of the Moon, i.e., the solid black curve, is no longer in the $\underline{xy}$-plane. Rather, the orbit of the Moon is projected onto the $\underline{xy}$-plane, as depicted a the dashed black curve. The equivalent Sun angle in the ephemeris force model is defined as the angle between two vectors. The

first vector is the vector directed from Earth to the projection of the Moon onto the ecliptic plane. The second vector from the Earth to the Sun is parallel to the -$\underline{x}$-axis. Given the definition of the Sun angle in the ephemeris model, a differential corrections algorithm is employed, that targets a specific Sun angle by varying the epoch date. A sample scenario is described as the closest full Moon, August 8^{th}, 2022. Using this technique, the algorithm predicts the nearest full Moon occurs on August 12^{th} at 01:37 UTC, just two minutes from the actual time of 01:35 UTC.

To generate an initial guess in the ephemeris force model, the states computed in rotating coordinate frames must be transitioned to an inertial reference frame. Recall, the equations of motion for the CR3BP and BCR4BP are modeled with nondimensional quantities. Both parameters used to dimensionalize the state vector explicitly rely on the distance between the primary bodies. Note that neither the Earth-Moon nor Sun-B_1 truly move in circular orbits in the ephemeris force model. Thus, the initial guess obtained from the BCR4BP varies depending on if the solution is rotated from the Earth-Moon or Sun-B_1 rotating reference frames. To account for this challenge, a pulsating strategy is employed. The states are dimesionalized via the appropriate quantities in the BCR4BP and CR3BP. As BLTs traverse between the Earth-Moon and Sun-B_1 systems, rotations from both rotating frames are applicable. A sample BLT is rotated into the Earth-centered J2000 inertial frame in Figure 17. The rotation process that originates in the Earth-Moon frame to the inertial coordinate frame is illustrated in Figure 17(a), while the rotation process beginning in the Sun-B_1 frame is in Figure 17(b). Boudad completed a similar analysis when constructing an initial guess for transfers between cislunar and heliocentric libration point orbits.[17] An important disclaimer is that neither Figure 17(a) or Figure 17(b) are actual trajectories in the ephemeris force model, rather, the algorithm shifts discrete position states along the path from the BCR4BP, and rotates them by employing a pulsating rotation strategy. Both Figure 17(a) and Figure 17(b) represent the same transfer from the BCR4BP in blue, while the black curve represents the motion of the Moon projected onto the XY-plane in inertial space. A key difference between the two rotation strategies is noticed near apogee, where Figure 17(a) depicts a lobe and two corners. In contrast, the transfer in Figure 17(b) appears more natural. The odd shape that occurs near apogee in Figure 17(a) is due to the eccentricity of the Moon's orbit with the distance and angular velocity near apogee. The origin of this behavior is likely from the pulsation of the different rotating frames. As the Earth-Moon system is elliptical, the distance between the Earth and the Moon changes by approximately 50,000 km or a $\pm 5\%$ change in characteristic length. For low-energy transfers that traverse over a million

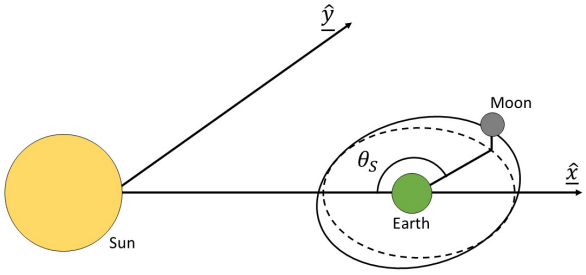

Figure 16: Schematic displaying the Sun angle as the angle between the Earth-Sun vector and the Earth-Moon vector projected onto the ecliptic plane

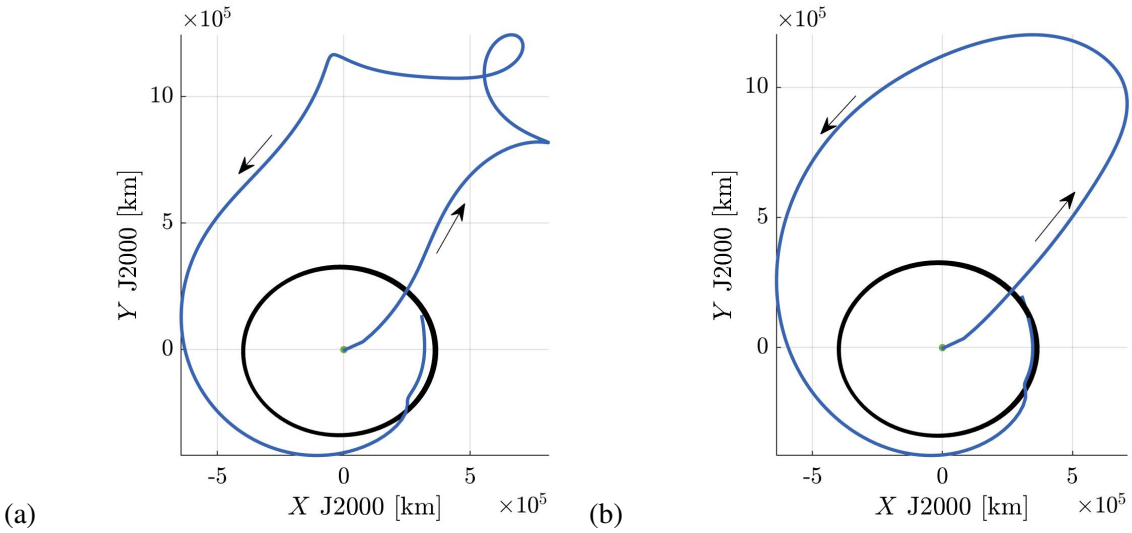

Figure 17: Rotating a BLT from the (a) Earth-Moon rotating frame and (b) Sun-B_1 rotating frame to Earth-centered J2000 inertial frame

kilometers from the Earth, a small adjustment in characteristic length magnifies at further distances. This pulsation is the source of the lobes in 17(a), since the spacecraft spends nearly a month near apogee. A similar pattern is apparent between the instantaneous mean motion of the Earth-Moon system and the rotated velocity components. From this observation, the rotation from the Sun-B_1 frame is more advantageous further from the Earth. The lower eccentricity of the Sun-Earth system and the longer timescales demonstrate a smaller influence on the rotation strategy. However, another minor difference is noted between Figure 17(a) and Figure 17(b). There is a slight variation in the rotated geometry when the transfers arrive in the lunar vicinity, i.e., approach the black curve. The Earth-Moon rotation strategy supplies an initial guess that generally align with the dynamical structures in the vicinity of the Moon. Since the Earth-Moon rotation incorporates the pulsation of the Moon, slight changes near the Moon aid in maintaining the complex dynamical structures apparent in the CR3BP and BCR4BP. Therefore, both rotation strategies are employed to construct BLTs in an ephemeris model. For all individual six-dimensional position and velocity states along the path within 200,000 km of the Moon, the Earth-Moon rotation method is applied to transition an initial guess in the Earth-centered J2000 frame. Otherwise, for states beyond 200,000 km from the Moon, the Sun-B_1 rotation strategy is utilized. This combined approach aids in transitioning these low-energy transfers from the CR3BP and BCR4BP to the ephemeris force model.

A family of low-energy transfers is constructed in the ephemeris force model. The family is selected from Figure 13, i.e., the set of transfers that evolve from a 150 km LEO to a L2 Lyapunov orbit. One advantage of this specific family is a solution that exists at every possible Sun angle, thus, there is an initial guess available for all epochs. To arrive into a Lyapunov orbit, the first step is construction of the destination orbits. Patch points from the selected CR3BP orbit are transitioned to the ephemeris model. The patch points are rotated from the Earth-Moon rotating frame into the Earth-centered inertial frame. Nine revolutions of the Lyapunov trajectory with five patch points per revolution are employed to maintain the geometry in ephemeris. The differential corrections technique targets continuity across all patch points. Once the periodic orbit is converged, 50 patch

points along the BLT are rotated into the Earth-centered inertial frame. The 50 states along the BLT are appended to the 45 points from the converged Lyapunov orbit, and the entire transfer is corrected for continuity. The only added constraints are the altitude and apse constraints. Recall these constraints require the initial state to be a perigee with an altitude of 150 km above the surface of the Earth. Otherwise, the targeter is solving for a ballistic path from Earth to the destination orbit. The transitioning process is repeated for 30 different solutions along the family from Figure 13, where each starting launch date is one day after the next. The family of BLTs in the ephemeris force model is represented in Figure 18. Each curve in Figure 18 departs the LEO on a different day in November 2024. After convergence in the Earth-centered inertial frame the transfers are rotated into a Sun-Earth rotating frame for comparison with the initial guess. By observing the geometry from the BCR4BP in Figure 13 to the ephemeris model in Figure 18, the overall structure remains. Another representation of the family is illustrated in Figure 19. Here the arrival Lyapunov orbit varies more widely in comparison to the solutions in the BCR4BP portrayed in Figure 14. As the entire transfer from the Earth to the orbit is ballistic, by incorporating small trajectory correction maneuvers along the path would offers additional control over the arrival multi-body orbit.

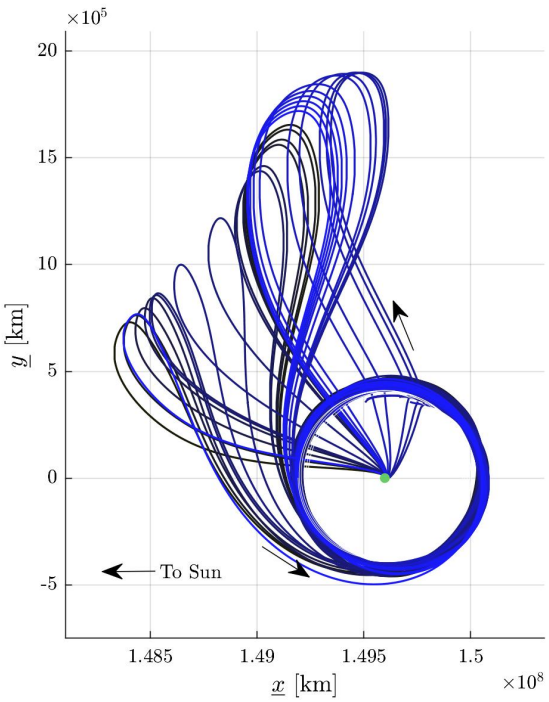

Figure 18: Family of BLTs from Figure 13 transitioned to the ephemeris force model, represented in the Sun-Earth rotating coordinate frame

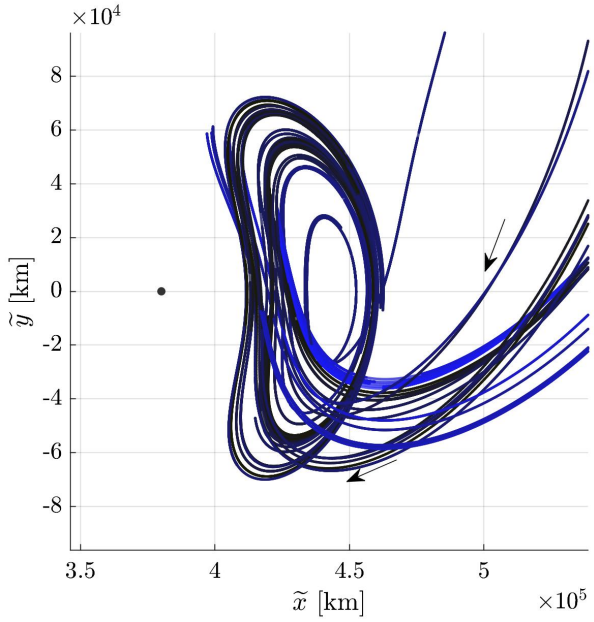

Figure 19: Family of BLTs from Figure 14 transitioned to the ephemeris force model, represented in the Earth-Moon rotating coordinate frame

CONCLUDING REMARKS

The CR3BP and BCR4BP offer effective models in constructing low-energy paths between the Earth and the Moon. The investigation expands upon previous analysis regarding transfers to conic orbits about the Moon. By analyzing potential mission objectives, families of transfers at different arrival LLOs are generated. The range of families offers insight into nearby transfer solutions and previously hidden structures. This analysis also explores a novel technique to generate BLTs that arrive in multi-body orbits, by combining the transfer portion in the BCR4BP to the the arrival conditions from the CR3BP. The approach enabled a low-energy transfer for any initial epoch. Lastly, strategies for transitioning BLTs to the ephemeris model are implemented. Incorporating work from a previous analysis,[17] initial epoch and rotation strategies are employed to construct end-to-end BLTs in the N-body ephemeris force model. Ultimately, this analysis demonstrates that low-energy transfers in the BCR4BP serve as an effective initial guess when transitioning solutions to a higher-fidelity model. The ability to leverage solar perturbations in the periodic model offers insight into the behavior and structure of low-energy transfers in cislunar and heliocentric space.

ACKNOWLEDGMENTS

The authors would like to thank the School of Aeronautics and Astronautics at Purdue University, and the Rune and Barbara Eliasen Visualization Laboratory for facilities and financial support. The authors would also like to thank Kenza Boudad, Brian McCarthy, and fellow members of the Purdue Multi-Body Dynamics Research Group for informative discussions. This work was completed under NSF Grant No. 10001485. The authors very much appreciate the support.

REFERENCES

[1] R. M. Smith, N. Merancy, and J. Krezel, "Exploration Missions 1, 2, and Beyond: First Steps Toward a Sustainable Human Presence at the Moon," *2019 IEEE Aerospace Conference*, Vol. 2019-, IEEE, 2019, pp. 1–12.

[2] N. L. Parrish, E. Kayser, S. Udupa, J. S. Parker, B. W. Cheetham, and D. C. Davis, "Ballistic Lunar Transfers to Near Rectilinear Halo Orbit: Operational Considerations," *AIAA Scitech 2020 Forum*.

[3] Y.-J. Song, Y.-R. Kim, J. Bae, J.-i. Park, S. Hong, D. Lee, and D.-K. Kim, "Overview of the Flight Dynamics Subsystem for Korea Pathfinder Lunar Orbiter Mission," *Aerospace*, Vol. 8, No. 8, 2021, 10.3390/aerospace8080222.

[4] S. Campagnola, J. Hernando-Ayuso, K. Kakihara, Y. Kawabata, T. Chikazawa, R. Funase, N. Ozaki, N. Baresi, T. Hashimoto, Y. Kawakatsu, T. Ikenaga, K. Oguri, and K. Oshima, "Mission Analysis for the EM-1 CubeSats EQUULEUS and OMOTENASHI," *IEEE Aerospace and Electronic Systems Magazine*, Vol. 34, 04 2019, pp. 38–44, 10.1109/MAES.2019.2916291.

[5] V. G. Szebehely, *Theory of Orbits: The Restricted Problem of Three Bodies*. New York: Academic Press, 1967.

[6] A. E. Roy, *Orbital Motion*. Bristol: A. Hilger, 2nd ed. ed., 1982.

[7] S. T. Scheuerle, "Construction of Ballistic Lunar Transfers in the Earth-Moon-Sun System," West Lafayette, Indiana, 2021. M.S. Thesis, Purdue University, West Lafayette, Indiana.

[8] C. H. Acton, "Ancillary data services of NASA's Navigation and Ancillary Information Facility," *Planetary and Space Science*, Vol. 44, No. 1, 1996, pp. 65–70. Planetary data system, https://doi.org/10.1016/0032-0633(95)00107-7.

[9] S. T. Scheuerle, B. P. McCarthy, and K. C. Howell, "Construction of Ballistic Lunar Transfers Leveraging Dynamical Systems Techniques," *AIAA/AAS Astrodynamics Specialist Conference*, August 2020.

[10] S. T. Scheuerle and K. C. Howell, "Characteristics and Analysis of Families of Low-energy Ballistic Lunar Transfers," *AIAA/AAS Astrodynamics Specialist Conference*, August 2021.

[11] T. H. Sweetser, "An estimate of the global minimum DV needed for earth-moon transfer," *Spaceflight Mechanics 1991*, Jan. 1991, pp. 111–120.

[12] D. C. Davis and K. C. Howell, "Characterization of Trajectories Near the Smaller Primary in the Restricted Problem for Applications," *Journal of Guidance, Control, and Dynamics*, Vol. 35, No. 1, 2012, pp. 116–128.

[13] J. S. Parker and G. H. Born, "Modeling a Low-Energy Ballistic Lunar Transfer Using Dynamical Systems Theory," Vol. 45, 2008, pp. 1269–1281.

[14] B. P. McCarthy and K. C. Howell, "Cislunar Transfer Design Exploiting Periodic and Quasi-Periodic Orbital Structures in the Four-Body Problem," *71th International Astronautical Congress*, 2020.

[15] B. P. McCarthy, "Cislunar Trajectory Design Methodologies Incorporating Quasi-Periodic Structures with Applications," *Ph.D. Dissertation*, West Lafayette, Indiana, 2022.

[16] E. M. Z. Spreen, "Trajectory Design and Targeting for Applications to the Exploration Program in Cislunar Space," *Ph.D. Dissertation*, West Lafayette, Indiana, 2021.

[17] K. K. Boudad, "Trajectory Design Between Cislunar and Sun-Earth Libration Points in a Four-body Model," *Ph.D. Dissertation*, West Lafayette, Indiana, 2022.